

# Thread inspired 3D printed clamps for in vitro biomechanical testing

---

Grgić, Ivan; Ivandić, Željko; Šotola, Dubravko; Kozak, Dražan; Karakašić, Mirko

Source / Izvornik: **Proceedings of TEAM 2018 9th International Scientific and Expert Conference, 2018, 45 - 53**

Conference paper / Rad u zborniku

Publication status / Verzija rada: **Accepted version / Završna verzija rukopisa prihvaćena za objavljivanje (postprint)**

Permanent link / Trajna poveznica: <https://urn.nsk.hr/urn:nbn:hr:262:376369>

Rights / Prava: [In copyright](#) / [Zaštićeno autorskim pravom](#).

Download date / Datum preuzimanja: **2025-03-26**



Repository / Repozitorij:

[repository.unisb.hr](https://repository.unisb.hr) - The digital repository is a digital collection of works by the University of Slavenski Brod.

# Thread inspired 3D printed clamps for in vitro biomechanical testing

I. Grgić <sup>a</sup>, Ž. Ivandić <sup>a</sup>, D. Šotola <sup>a</sup>, D.Kozak <sup>a</sup>, M.Karakašić <sup>a</sup>

<sup>a</sup> Mechanical Engineering Faculty in Slavonski Brod, Trg I. B. Mažuranić 2, 35000 Slavonski Brod, Croatia, igrbic@sfsb.hr

## Abstract

In recent biomechanical testing of soft tissues, many researchers have presented the usage of different clamping techniques such as using frozen clamps, non-frozen serrated jaw clamps, a non-frozen clamp which has lateral block boards and asymmetrical teeth jaws to prevent tissues from slipping and without damaging it at high loads. In this study, for future biomechanical testing of human gracilis and quadriceps tendons, we present the usage of a 3D printing approach as a possibility for making clamps. We took the measures of the existing pneumatic jaw clamps on Shimadzu AGS-X 10 kN machine and according to the measurements, we have designed and 3D print the clamps which have different geometry inspired by the cross-sectional view of metric, trapezoidal and buttress thread, to act as extensions to existing ones and to be able to prevent tendon slipping and damaging during compression. Based on the tensile tests using porcine tendons, we report our experience. It has been shown that we can avoid expensive changes in existing equipment, buying commercially available plastic and metal materials and manufacturing it or else use frozen clamps which are complex and expensive. We have shown that using a low-cost 3D printer and cheap polyethylene terephthalate glycol (PET-G) material can lead to successful scientific work. To our knowledge, by searching available literature, there is only one similar study published during writing this paper.

**Keywords:** Biomechanical testing, 3D printed clamp, Superficial flexor tendon, Thread.

## 1. INTRODUCTION

Because of soft tissue viscoelastic characteristics and low friction between the clamp material and wet soft tissues, it is difficult to hold them rigidly at in vitro loads and loading speed. Excessive compression on the soft tissue will elevate stress around the contact area, which leads to rupture before target loads are achieved, too little compression will result in slippage [1]. First successful attempt to prevent above-mentioned problems was solved with „cryo-jaw“ clamp presented in 1982. by Riemersa and Schamhardt [2]. They use clamps made of brass which can be connected together with four M8

screws to compress the tendon ends and then freezing with circulating liquid carbon dioxide. Sharky et al. [3] have applied a similar method on quadriceps and Achilles tendons without slippage and no problems with compression. Schatzman et al. [4] used water in the containment chamber, waited for the water to be frozen and then they proceed with testing of human quadriceps tendon-bone complexes and patellar ligament-bone complexes. Due to complex freezing equipment, other researches have reported some different solutions. Cheung and Zhang [5] presented non-frozen serrated yaw clamp made of serrated plastic material. Ng et al. [6] have tested the several gripping methods and evaluated

them, including serrated jaw, sandpaper, frozen ends and air-dried ends on 1 kN Shimadzu pneumatic grips and it was found that using the pneumatic grips with cardboard lining the stress concentration at the grip-specimen interface reduced substantially. During writing this paper one similar approach has been published [7]. In that paper, authors use quasi-static tensile tests combined with digital image correlation and fatigue trials characterized the applicability of the clamping technique using 3D printed clamps. They have reported that 3D printed clamps showed no signs of clamping-related failure during the quasi-static tests and in the fatigue tests, material slippage was low, allowing for cyclic tests beyond  $10^5$  cycles. Comparison to other clamping techniques yields that 3D printed clamps ease and expedite specimen handling, are highly adaptable to specimen geometries and ideal for high-standardization and high-throughput experiments in soft tissue biomechanics. They used clamp design with 4-sided pyramid structures in cross-sectional view. For all 3D prints, the parts were produced with 100-micron layers using a 0,4 mm brass nozzle. The clamps were printed in an upright position for a lateral orientation of the pyramids, allowing a very detailed quality of these surface structures. The material used for 3D printing of clamps was polylactic acid (PLA). In this study, we report our preliminary experience using a 3D printing technique for the future biomechanical tests of human gracilis and quadriceps tendons. This approach is based on the analysing and measuring of the parts of the existing equipment, 3D modelling, 3D printing, mounting on the machine, testing and validation. All parts of the approach will be discussed.

## 2. METHODS AND MATERIALS USED FOR RESEARCH

### 2.1. Analysis and measurement of 10 kN Shimadzu pneumatic grips

After reassembling the lower pneumatic grip as shown in Figure 1, from the 10 kN Shimadzu tensile test machine, we proceed with the analysis and measurement of grip parts. It has been

determined that clamps have next properties: 40x60x10 mm, two holes with M4x1 mm internal thread, 4 mm deep, while the hole is 7 mm deep. The middle hole is 16 mm in diameter and 4 mm deep. Figure 2 shows all the other properties. The same procedure has been done for the upper pneumatic grip and clamps. We also have to take care of space between the two pneumatic clamps to see how much space do we have for 3D printed clamps.

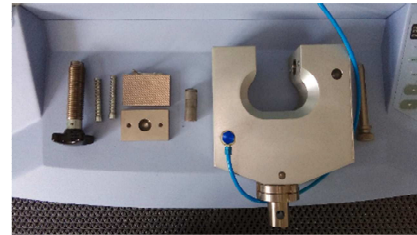


Fig. 1. Parts of the lower pneumatic grip

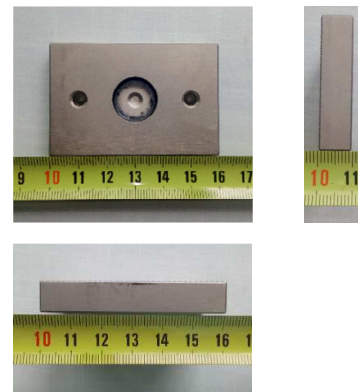


Fig. 2. Orthogonal projections

### 2.2. 3D model of clamps

When we look at the side view of the clamp, we considered it as a cross-sectional view of a one half of a bolt, which means that the clamp thickness of 10 mm represents one half of a bolt. If we add the additional material, in this case, PET-G clamps, the thickness will rise. To conclude, we act like we have a bolt which has 40 mm in diameter and according to that, we have to choose appropriate metric M42x4,5 mm (M40 is not listed into a group of normal metric threads by the literature), trapezoidal Tr40x3mm and buttress S40x3mm external thread according to DIN 103. Therefore, using SolidWorks 2016, we put the “bolt” axis on one side of the clamp and on the other we have added thread profile. This procedure is shown in Figure 3 and an example

of the complete 3D model in Figure 4. For 3D printing, all models were exported as a *.stl* file.

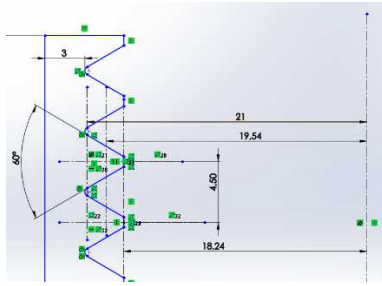


Fig. 3. Metric thread design

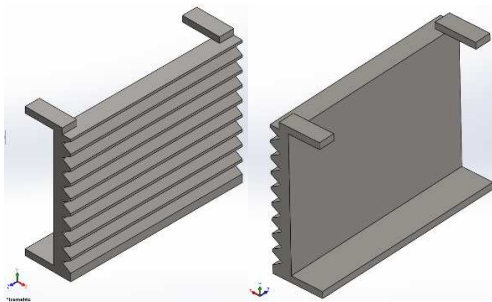


Fig. 4. 3D model of clamps (front and back isometric view)-metric thread

### 2.3. 3D printing and mounting

All models were processed with the Ultimaker Cura 3.4.1 slicing application before printing and Creality Ender-2 3D printer was used. All models were printed in the upright position with polyethylene terephthalate glycol (PET-G) commercially available biodegradable material with 200-micron layers and 0,4mm brass nozzle, Figure 5. The temperature of the nozzle was set to 225 °C and 60 °C for the bed. Figure 5 shows the example of a 3D printed clamp with a buttress thread during the printing process.

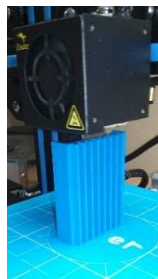


Fig. 5. Clamp during printing with buttress thread design

Next step was mounting 3D printed clamps on the pneumatic grips, which is shown here in Figure 6.



Fig. 6. Mounted clamps

### 2.4. Biomechanical tests

Forty-two porcine superficial flexor tendons were obtained from an abattoir within two hours after sacrifice. After removing all connective tissue, the tendons were finally isolated and stored in airtight plastic bags and put in the freezer at -20 °C. Before testing, the specimens were thawed in the water while they still left in their plastic bags to avoid contact with the water during the thawing process which has lasted around 30 minutes. Each specimen was dried out with a soft rag to remove surface moisture. 14 specimens were randomly selected for each of the three clamping methods since we have differences in their length and we intentionally do not want to cut them on the same length. In conclusion, we want random test without forcing anything. Seven of them left in its natural shape and seven of them were formed in dog-bone shape per each clamp. To form the dog-bone shape cutting area was marked. Subsequently, five markers were put on the specimen surface, three of them to serve as guide-points for cutting curves and other two for tracking eventual slippage. The procedure is shown in Figure 7 and finally shape in Figure 8.

The same procedure was used for the tendons which were left in their natural shape, of course without dog-bone cutting paths. For each specimen, the length and cross-sectional area were measured 5 times and the mean value was used.



*Fig. 7. Markers on the specimen*



*Fig. 8. The final shape of the specimen(dog-bone)*

Then the specimens were mounted on the tensile test machine. The gauge length was measured and it was approximately 35 mm long. The pressure applied to the grips were set to 3 bar (720 N clamping force). To reduce tissue hysteresis, the specimens were preloaded with a force of 2 N and preconditioned by a series of 10 cycles starting from the undeformed position (0 mm) up to the stroke of 1,5 mm with a stroke rate of 10 mm/min. Five minutes after the preconditioning phase, tendons were tested until their failure. First, they were preloaded with a force of 2 N to remove slack, zero force and movement were established and the test started with 10 mm/min of stroke rate until specimen failure. Example of the experimental setup is presented in Figure 9 with a tendon in its natural form.

The mean values of the ultimate tensile strength (UTS), ultimate stroke strain, and structural modulus were measured. Note that the structural modulus and ultimate stroke strain differ from the actual elastic modulus and ultimate strain of the tendon as they are based on the cross-head motion of the grips. However, for relative comparison between different grips, these can be used [6].

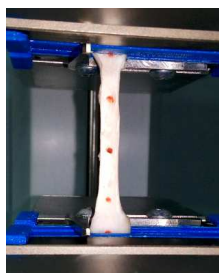


*Fig. 9. Setup of the experiment*

### 3. RESULTS AND ACHIEVEMENTS

All presented data have been extracted from the Trapezium X software.

#### 3.1. Trapezoidal clamps

All tests which include dog-bone shaped specimens were finished without slipping and there were no specimen ruptures in the clamping area. Also, all specimens failed in their mid-substance, and an example is shown in Figure 10. Among seven natural shaped specimens, one specimen failed in its mid-substance and three specimens failed at the place where specimen leaves the clamping area. Smith et al. [8] compared the mean ultimate tensile strength of tendons failing at the clamp with the mean ultimate tensile strength of those failing in the mid-substance and found no significant difference between the ultimate tensile strength of ‘clamp failures’ and the ‘mid-failures’. They suggested that the data from clamp failure tests could also be included with data from mid-failure tests [6]. Slippage of 10 mm and rupture in the clamping area occurred in three specimens tested in its natural form, an example is presented in Figure 11. It was excluded from further observations. The recorded mean value of the ultimate tensile strength (UTS) was  $50,16 \pm 13,51$  MPa, ultimate stroke strain  $30,04 \pm 6,10$  % and structural modulus  $254,73 \pm 68,24$  MPa. Results for the naturally shaped specimens were as follows, the mean value of ultimate tensile strength (UTS) was  $34,78 \pm 9,11$  MPa, ultimate stroke strain  $32,29 \pm 7,57$  % and structural modulus  $160,31 \pm 50,94$  MPa. It can be noticed that the difference of 30,66 % is between ultimate tensile strengths, 7,49 % between ultimate stroke strains, and 37,06 % between structural modulus results. Results are also presented below in Figures 12 and 13. Typical tendon tensile test curves and the last tenth cycle of hysteresis are shown in Figures 14, 15, 16 and 17.



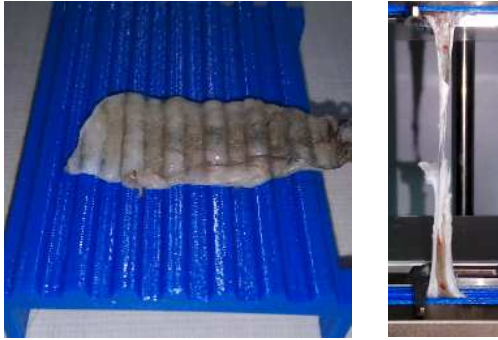


Fig. 10. Clamping area and mid-substance failure of the specimen after the tensile test

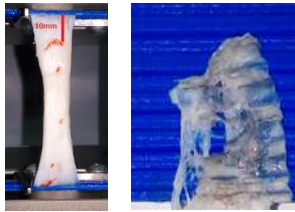


Fig. 11. Slippage of 10 mm and rupture

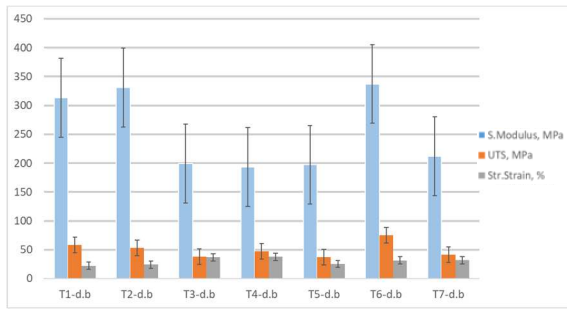


Fig. 12. Results of dog-bone shaped specimen

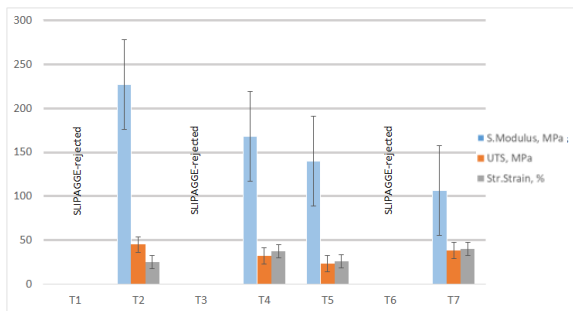


Fig. 13. Results of specimens in their natural form

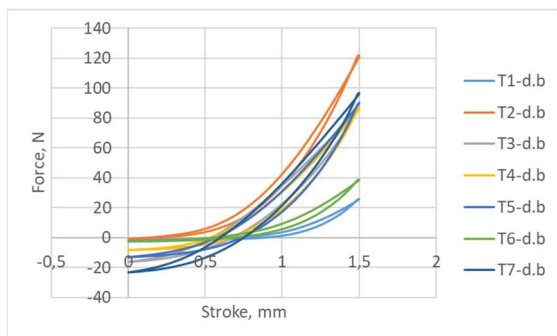


Fig. 14. Hysteresis curves of dog-bone specimens

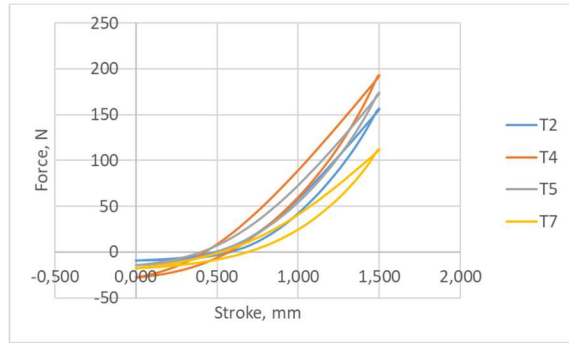


Fig. 15. Hysteresis curves of specimens in natural form (specimens T1, T3, T6 rejected)

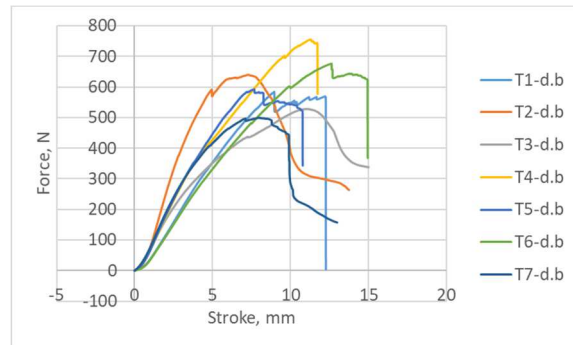


Fig. 16. Tensile tests of dog-bone specimens

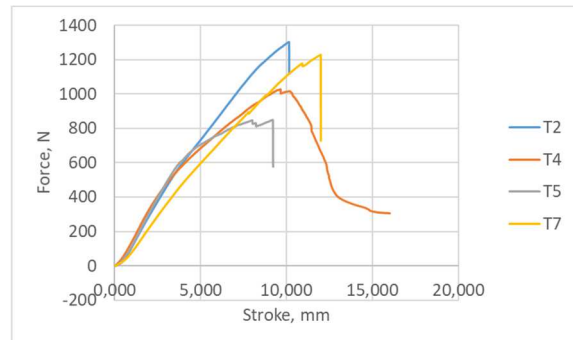


Fig. 17. Tensile tests of specimens in their natural form (specimens T1, T3, T6 rejected)

### 3.2. Metric clamps

One test of the dog-bone shaped specimen was finished by slipping, three of them were failed in the mid-substance and also three of them at a clamp where tendon leaves the clamping area. There were no specimen ruptures found. Among seven natural shaped specimens, two specimens failed in its mid-substance and three specimens failed at the place where specimen leaves the clamping area. Slipping of 2 mm occurred in two tests without ruptures and they were excluded from the analysis.

The recorded mean value of the ultimate tensile strength (UTS) was  $41,68 \pm 5,39$  MPa, ultimate

stroke strain  $23,74 \pm 3,66$  % and structural modulus  $236,09 \pm 66,50$  MPa. Results for the naturally shaped specimens were as follows, the mean value of ultimate tensile strength (UTS) was  $41,12 \pm 6,44$  MPa, ultimate stroke strain  $22,49 \pm 3,31$  % and structural modulus  $104,98 \pm 47,14$  MPa. It can be noticed that the difference of 0,86 % is between ultimate tensile strengths, 5,26 % between ultimate stroke strains, and 55,53 % between structural modulus results. Results are also presented below in Figures 18 and 19. Typical tendon tensile test curves and the last tenth cycle of hysteresis are shown in Figures 20, 21, 22 and 23.

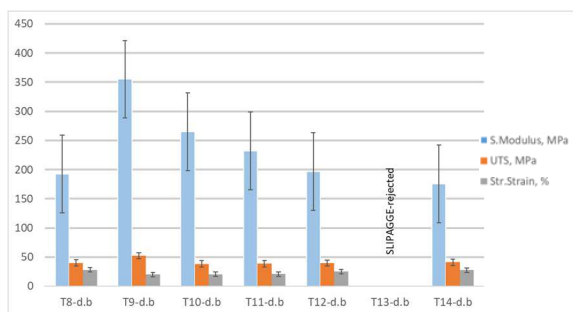


Fig. 18. Results of dog-bone shaped specimen

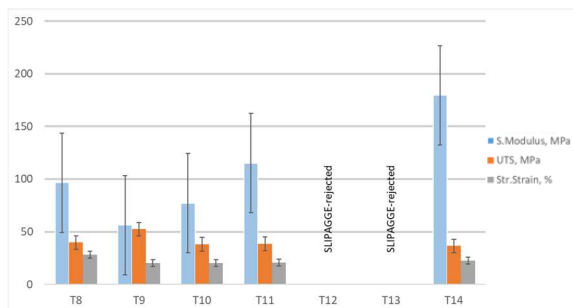


Fig. 19. Results of specimens in their natural form

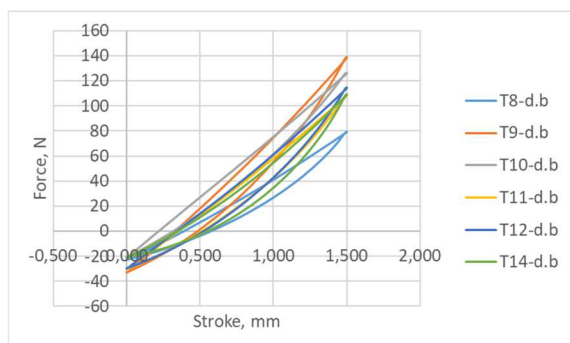


Fig. 20. Hysteresis curves of dog-bone specimens (T13-d.b rejected)

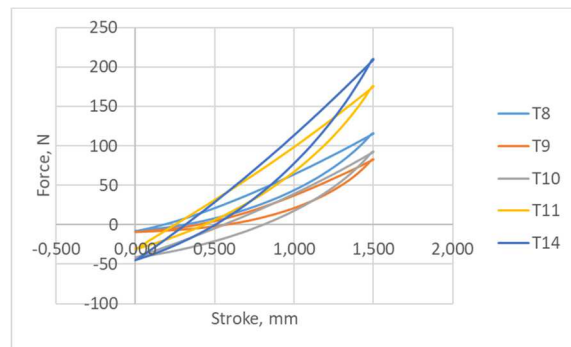


Fig. 21. Hysteresis curves of specimens in natural form (specimens T12, T14 rejected)

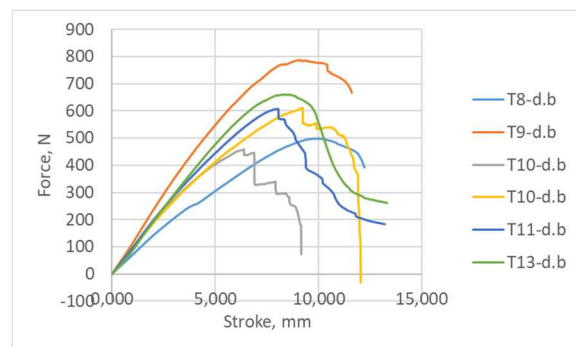


Fig. 22. Tensile tests of dog-bone specimens (T12-d.b rejected)

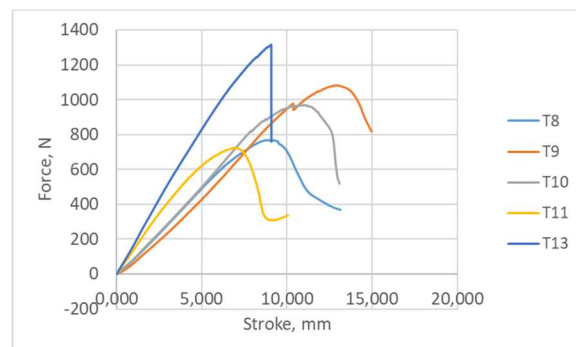


Fig. 23. Tensile tests of specimens in their natural form (specimens T1, T3, T6 rejected)

### 3.3. Buttress clamps

Among seven dog-bone shaped specimens, one was excluded due to slipping and one because it had bad geometry (cuts caused by imprecise dissection). Four of the specimens failed at its mid-substance and the last one failed at the place where tendon exits the clamping area. Two slipping and rupturing cases in clamping area occurred in two specimens tested in its natural form and they were also excluded from the analysis. Slippage was 3 mm long. The recorded mean value of the ultimate tensile strength (UTS) was  $55,73 \pm 3,96$  MPa, ultimate

stroke strain  $24,31 \pm 3,96$  % and structural modulus  $304,62 \pm 48,92$  MPa. Results for the naturally shaped specimens were as follows, the mean value of ultimate tensile strength (UTS) was  $30,75 \pm 16,79$  MPa, ultimate stroke strain  $26,29 \pm 2,05$  % and structural modulus  $108,04 \pm 53,81$  MPa. It can be noticed that the difference of 44,82 % is between ultimate tensile strengths, 8,14 % between ultimate stroke strains, and 64,53 % between structural modulus results. Results are also presented below in Figures 24 and 25. Typical tendon tensile test curves and the last tenth cycle of hysteresis are shown in Figures 26, 27, 28 and 29.

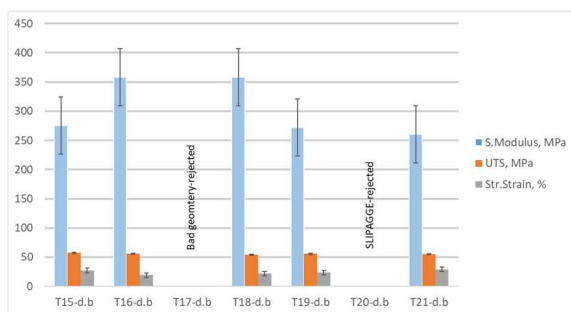


Fig. 24. Results of dog-bone shaped specimen

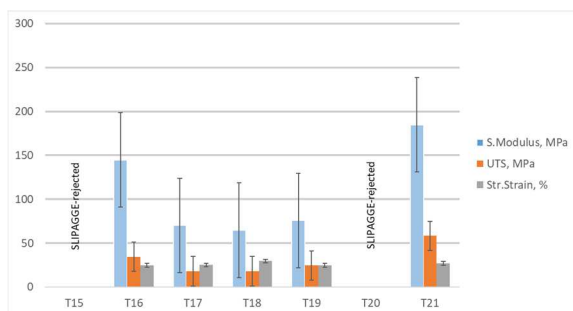


Fig. 25. Results of specimens in their natural form

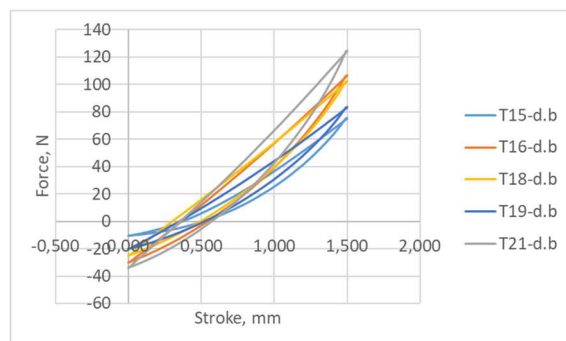


Fig. 26. Hysteresis curves of dog-bone specimens (T17-d.b, T20-d.b rejected)

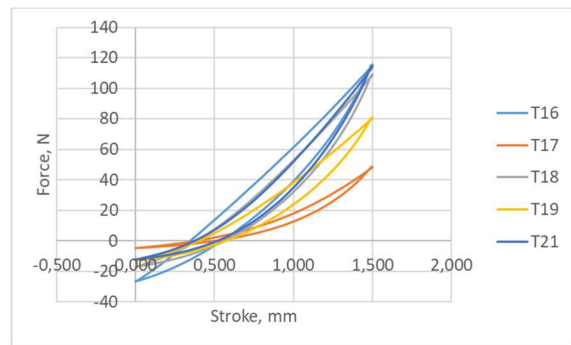


Fig. 27. Hysteresis curves of specimens in natural form (T15, T20 rejected)

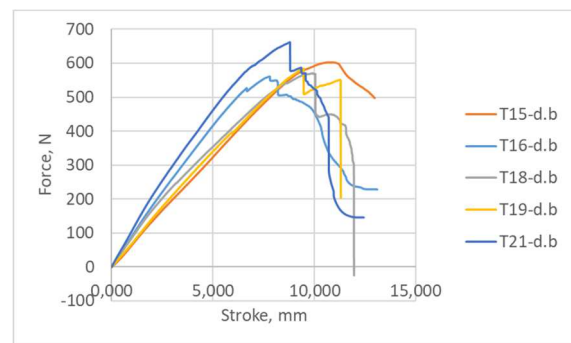


Fig. 28. Tensile tests of dog-bone specimens (T17-d.b, T20-d.b rejected)

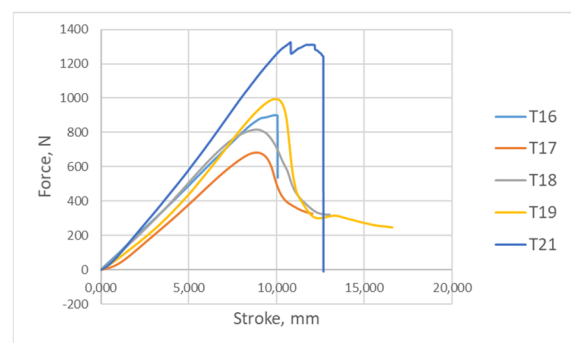


Fig. 29. Tensile tests of specimens in their natural form (specimens T15, T20 rejected)

### 3.3. Discussion

The average 3D printing time was 2 hours and 15 minutes per clamp. The infill was set to 100%. During printing, we did not have any issues. Clamps fit extremely well at their places on the tensile test machine. The only problem that we had was the easily horizontal movement which causes the small problem during mounting of specimens. During writing this paper, one similar approach was published and it was shortly described above in the introduction, we will consider their approach and find something



suitable solution for our mounting problem. We choose to use the clamping pressure of 3 bar and it shows good clamping behaviour during tests and we found no damage after all. In the [7] they used 6 bar. Maybe we should consider the bigger amount of pressure for the future tests to reduce slipping but it could result in higher stress concentrations in tendons tissue and more ruptures in clamping area as well. After all, we did not find any damage in the clamping area or at any other place over the clamps, which indicates that they are very reusable.

Tendons length average was 90 mm, thickness average was 4 mm and width average was 8 mm with an elliptical shape of the cross-sectional area. For testing of tendons in their natural form, we had assumed that we have a rectangular cross-sectional area. While creating dog-bone shaped specimen, inspired by sample preparation in [9], in some cases we had problems to achieve well-shaped cross-sectional area, so we should have in mind to use or to create some special tool which could help us with this issue. Still, by searching available literature, there is no clear statement about either to test tendons by creating a dog-bone shape or either to test them in their natural form and also there are no concrete statements about testing protocol. To avoid possible corrosion appearance at our equipment we could not prevent tendons from dehydration by spraying them during tests. We proceed with hysteresis tests and tensile tests. Our rejection term was if a tensile test fails then we will exclude hysteresis results as well. To be clear, we could use them since there is no slippage or rupture because of small loads and displacements but we want 100 % success with tensile tests. We also want to proceed with creep and stress-relaxation tests and fatigue tests as well, but since they are long-lasting tests and since we could not provide tissue moistening, we gave up. Since we have mentioned above disadvantages of this work and the small sample size per one clamp we do not provide any statistical conclusions. But if one may ask us to choose which clamp design could be better to use among others, we will recommend trapezium clamps for samples with dog-bone shaped tendons and then clamps with

buttress thread. By our experience, the metrical clamps should be used only for testing tendons in their natural form because these are the only clamps at which failure occurred in mid-substance. To conclude, the complete review of the average values of tissue properties between types of clamps are given in Figure 30.

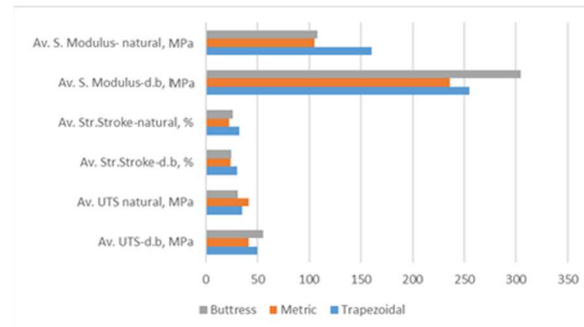


Fig. 30. Average tendon properties and types of clamps

The key advantages of the 3D printed clamps are the ease of use, adaptability, reusability, modularity and the fact that they can be manufactured easily and at local research environments. Furthermore, recent developments in prices, usability and variety of desktop FDM-printers (which was used in this study) allow easy integration into laboratory environments. Without the maintenance time of the printer, which is often reduced to some minutes (when changing a filament spool or cleaning the build-plate), no additional working time is required for the manufacturing of the parts for testing. Geometries and print settings can be shared easily, forming a basis for affordable add-ons to existing testing devices for tissue biomechanics [7].

Based on this study, in the future, we aim to develop clamps suitable for the existing equipment and be able to work in special environmental conditions to simulate human body environment and also to avoid above-mentioned slipping and compression problems. We want to provide the standardized, specially designed clamps for soft tissue testing. Our future tests will also be based on porcine tendons and later on human gracilis and quadriceps tendons.

We will involve some additional methods such as digital image correlation, methods to prevent tissue dehydration, etc., to help us in the determination of biomechanical properties which will not be based on cross-head movement and not be classified as structural. We will consider a bigger sample size to provide statistically based conclusions. Also, we will try some different clamp pattern instead of thread design based clamps and different material such as polylactic acid (PLA) or thermoplastic polyurethane (TPU).

#### Acknowledgement

The authors acknowledge the support of local slaughterhouse Bebrinka d.o.o for the donation of porcine tendons, especially to Ivica Mirković, head of the slaughterhouse and to Slavica Baboselac, the technologist at the slaughterhouse.

#### 4. REFERENCES

- [1] A. Arndt, P. Kom, G.-P. Brüggemann & J. Lukkariniemi, »Individual muscle contributions to the in vivo Achilles tendon force,« *Clinical Biomechanics*, pp. 532-541, 1998.
- [2] D. J. Riemersma & H. C. Schamhardt, »The cryo-jaw, a clamp designed for in vitro rheology studies of horse digital flexor tendons,« *Journal of biomechanics*, pp. 619-620, 1982.
- [3] N. A. Sharky, T. S. Smith & D. C. Lundmark, »Freeze clamping musculotendinous junctions for in-vitro simulation of joint mechanics,« *Journal of Biomechanics*, pp. 631-635, 1995.
- [4] L. Schatzmann, P. Brunner & H. U. Staubli, »Effect of cyclic preconditioning on the tensile properties of human quadriceps tendons and patellar ligaments,« *Knee surgery, sports traumatology, arthroscopy*, pp. 56-61, 1998.
- [5] J. T. M. Cheung & M. A. Zhang, »A serrated jaw clamp for tendon gripping,« *Medical Engineering & Physics*, pp. 379-382, 2006.
- [6] B. H. Ng, S. M. Chou & V. Krishana, »The influence of gripping techniques on the tensile properties of tendons,« *Journal of engineering in medicine*, pp. 349-354, 2005.
- [7] M. Scholze, A. Singh, P. F. Lozano, B. Ondruschka, M. Ramezani, M. Werner & N. Hammer, »Utilization of 3D printing technology to facilitate and standardize soft tissue testing,« *Scientific Report*, pp. 1-8, 27 7 2018.
- [8] C. W. Smith, L. S. Young & J. N. Kearny, »Mechanical properties of tendons: changes with sterilization and preservation,« *J. Tensile Engng*, pp. 56-61, 1996.
- [9] A. Herbert, G. L. Jones, E. Ingham & J. Fisher, »A biomechanical characterisation of acellular porcine super flexor tendons for use in anterior cruciate ligament replacement: Investigation into the effects of fat reduction and bioburden reduction bioprocesses,« *Journal of Biomechanics*, pp. 22-29, 2015.
- [10] K. Smeets, J. Bellemans, L. Scheys, B. O. Eijnde, J. Slane & S. Claes, »Mechanical Analysis of Extra-Articular Knee Ligaments: Part two: Tendon grafts used for knee ligament reconstruction,« *The Knee*, pp. 1-8, 2017.